MNRAS **000**, 000–000 (0000) Preprint 11 May 2018 Compiled using MNRAS LATEX style file v3.0

Temperature-dependent oscillation modes in rotating superfluid neutron stars

V. A. Dommes, E. M. Kantor, M. E. Gusakov
Ioffe Institute, Polytekhnicheskaya 26, 194021 St. Petersburg, Russia

11 May 2018

1 INTRODUCTION

According to the standard r-mode theory, hot and rapidly rotating neutron stars (NSs) in low-mass X-ray binaries (LMXBs) should be CFS-unstable with respect to emission of gravitational waves (Andersson 1998; Friedman & Morsink 1998). As a consequence, the probability to observe them should be very small, but this conclusion contradicts observations (Ho et al. 2011). There has been proposed a number of possible solutions to this paradox (see, e.g. Andersson & Kokkotas 2001; Haskell et al. 2012; Ho et al. 2011; Mahmoodifar & Strohmayer 2013), but it still remains an open problem. Gusakov et al. (2014a,b) introduced a new scenario, in which the finite-temperature effects in the superfluid core of an NS lead to resonance coupling and enhanced damping (and hence stability) of oscillation modes at certain "resonance" stellar temperatures. It was demonstrated that NSs in LMXBs with high spin frequency may spend a substantial amount of time at these resonance temperatures, so their interpretation does not constitute a problem.

The proposed scenario was based on a simplified phenomenological model (in particular, resonance temperatures have never been calculated explicitly). To put in on a more solid ground, one has to calculate for realistic superfluid NS models spectrum of rotational inertial modes (modes for which the restoring force is Coriolis force) at arbitrary temperatures in order to find resonance temperatures at which the normal r-mode exhibits an avoided crossing with some another mode. However, in most of works (e.g. Lindblom & Mendell 2000; Prix et al. 2002; Lee & Yoshida 2003; Andersson et al. 2009) the inertial modes are studied only in zero-temperature limit, when all neutrons and protons are assumed to be in superfluid state.

Kantor & Gusakov (2017) considered normal and superfluid r-modes, taking into account finite-temperature effects and stratification by muons (μ) and found avoided crossings between normal and superfluid r-mode in the next-ot leading order in stellar rotation frequency. This work ignored the entrainment between superfluid neutrons and protons, which significantly affects the spectrum of superfluid inertial modes (see, e.g. Lee & Yoshida 2003). Also Kantor & Gusakov (2017) focused only on r-modes and have not studied other inertial modes, which also can interact with the normal r-mode. To fill this gap, we calculate the spectrum of inertial modes in superfluid NSs whose cores consist of neutrons (n), protons (p) and electrons (e), accounting for both entrainment and finite-temperature effects. We present the first results of such calculations, obtained under assumptions of *npe* NS core composition and constant critical temperatures. Section 4 presents the results of these calculations. In Section 5 we also present an approximate method that allows to calculate the superfluid r-mode analytically, in the limit of small entrainment. In Section 6 we derive dispersion relations for inertial modes in superfluid *npe* matter in short-wavelength limit, and explain some properties of these modes that can be observed in the numerical results calculated in Section 4. Finally, we sum up in Section 7.

2 EQUATIONS GOVERNING OSCILLATIONS OF A ROTATING NS

Using the Newtonian limit of the relativistic hydrodynamics, formulated by Gusakov (2016); Gusakov & Dommes (2016), and describing rotating superfluid mixture at a finite temperature, we consider small oscillations of a slowly rotating (with the spin frequency Ω) NS in the Cowling approximation. Let all the quantities depend on time t as $\mathrm{e}^{\imath\sigma t}$ in the coordinate frame rotating with the star (with frequency Ω). Then the linearised equations governing small oscillations of superfluid (hereafter SFL) NSs in that frame are:

(i) Euler equation

$$-\sigma^2\boldsymbol{\xi}_{\rm b}+2\imath\sigma\boldsymbol{\Omega}\times\boldsymbol{\xi}_{\rm b}=\frac{\delta w}{w^2}\boldsymbol{\nabla}P-\frac{\boldsymbol{\nabla}\delta P}{w}, \tag{1}$$

where $w=(P+\epsilon)/c^2$, P is pressure, ϵ is energy density, c is speed of light. Here and hereafter, δ stands for its Euler perturbation (e.g., δP). Finally, $\boldsymbol{\xi}_{\rm b}$ is the Lagrangian displacement of baryons, it is defined as $\boldsymbol{\xi}_{\rm b}\equiv\boldsymbol{\jmath}_{\rm b}/(\imath\sigma n_{\rm b})$, where $n_{\rm b}\equiv n_{\rm n}+n_{\rm p}$ and $\boldsymbol{\jmath}_{\rm b}\equiv\boldsymbol{\jmath}_n+\boldsymbol{\jmath}_p$ are the baryon number density and baryon current density, respectively.

(ii) Continuity equations for baryons and electrons

$$\delta n_{\rm b} + \mathrm{div}(n_{\rm b}\boldsymbol{\xi}_{\rm b}) = 0, \quad \delta n_{\rm e} + \mathrm{div}(n_{\rm e}\boldsymbol{\xi}) = 0. \tag{2}$$

Here $\boldsymbol{\xi} \equiv \boldsymbol{\jmath}_e/(\imath\sigma n_{\rm e})$ is the Lagrangian displacement of the normal liquid component[1], and $n_{\rm e}$ is the electron number density. Note that if neutrons are non-superfluid, then $\boldsymbol{\xi} = \boldsymbol{\xi}_{\rm b}$ and hydrodynamic equations become essentially the same as in the normal matter even if protons are superfluid (e.g. Gusakov & Andersson 2006).

(iii) The 'superfluid' equation, analogue of the Euler equation for superfluid (neutron) liquid component

$$h\sigma^2\boldsymbol{z} - 2\imath h_1\sigma\boldsymbol{\Omega}\times\boldsymbol{z} = c^2 n_{\rm e}\boldsymbol{\nabla}\Delta\mu_{\rm e} \tag{3}$$

where $\boldsymbol{z} \equiv \boldsymbol{\xi}_{\rm b} - \boldsymbol{\xi}$ is the superfluid Lagrangian displacement; and $\Delta\mu_{\rm e} \equiv \mu_{\rm n} - \mu_{\rm p} - \mu_{\rm e}$ is the chemical potential imbalance (note that in equilibrium $\Delta\mu_{\rm e} = 0$, thus $\delta\Delta\mu_{\rm e} = \Delta\mu_{\rm e}$); Furthermore,

$$h = n_{\rm b}\mu_{\rm n} y, \quad h_1 = \mu_{\rm n} n_{\rm b}\left(\frac{n_{\rm b}}{Y_{nk}\mu_k} - 1\right), \quad y = \frac{n_{\rm b} Y_{\rm pp}}{\mu_{\rm n}(Y_{\rm nn}Y_{\rm pp} - Y_{\rm np}^2)} - 1, \tag{4}$$

here μ_k is the chemical potential of neutrons ($k = n$) and protons ($k = p$), Y_{ik} (indices i, k run over neutrons and protons) are elements of the entrainment matrix (see, e.g., Gusakov et al. 2014c) analog of the superfluid density for relativistic mixtures. In Eq. (4) summation over $k = n$, p is assumed. Superfluid equation in the form (3) is valid only the interaction between the neutron vortices and normal component (e.g., electrons) is weak (so-called weak-drag regime) which is a typical situation in NS cores (see, e.g. Mendell 1991; Andersson et al. 2006).

The above equations should be supplemented by the 'equation of state' (EOS), $\delta n_i = \frac{\partial n_i}{\partial P}\delta P + \frac{\partial n_i}{\partial \Delta\mu_{\rm e}}\Delta\mu_{\rm e}$.

In the present study we are interested in the oscillations, which have the eigenfrequencies σ vanishing at $\Omega \to 0$. Thus, up to the terms $\sim (\Omega/\Omega_0)^2$ (Ω_0 is of the order of Kepler frequency), the eigenfrequency σ, the Euler perturbation of any (scalar) thermodynamic parameter f (e.g., P, $\mu_{\rm e}$, $n_{\rm b}$, etc.), and the Lagrangian displacement $\boldsymbol{d}$ (e.g., $\boldsymbol{\xi}_{\rm b}$ or $\boldsymbol{z}$) can be presented as (Lockitch & Friedman 1999)

$$\sigma = \Omega\sigma_0\left(1 + \Omega^2\sigma_1\right), \tag{5}$$

$$\delta f = \Omega^2 \delta f^1 \exp(\imath\sigma t + \imath m\phi), \tag{6}$$

$$\boldsymbol{d} = \left(\boldsymbol{d}^0 + \Omega^2\boldsymbol{d}^1\right)\exp(\imath\sigma t + \imath m\phi) \tag{7}$$

where m is integer and ϕ is the azimuthal angle.

Here we work only to the leading order in Ω/Ω_0, i.e. ignore σ_1, $\boldsymbol{d}^1$ and the star oblateness (i.e. all equilibrium values depend on the radial coordinate only). In this order system (i)-(iii) can be written in spherical coordinates as

$$-\sigma_0^2\xi^0_{\rm br} - 2\imath\sigma_0\sin\theta\xi^0_{{\rm b}\phi} = -\frac{\partial}{\partial r}\frac{\delta P^1}{w_0} + \frac{\mu_{\rm n}}{w_0^2 c^2}\frac{\partial n_{\rm b}}{\partial\Delta\mu_{\rm e}}\Delta\mu_{\rm e}^1\frac{dP_0}{dr}, \tag{8}$$

$$-\sigma_0\xi^0_{{\rm b}\theta} - 2\imath\cos\theta\xi^0_{{\rm b}\phi} = \frac{1}{\imath m}\frac{\partial}{\partial\theta}\sin\theta\left[-\sigma_0\xi^0_{{\rm b}\phi} + 2\imath\left(\xi^0_{\rm br}\sin\theta + \xi^0_{{\rm b}\theta}\cos\theta\right)\right], \tag{9}$$

$$-\sigma_0^2\xi^0_{{\rm b}\phi} + 2\imath\sigma_0\left(\xi^0_{\rm br}\sin\theta + \xi^0_{{\rm b}\theta}\cos\theta\right) = -\frac{1}{w_0}\frac{\imath m}{r\sin\theta}\delta P^1, \tag{10}$$

$$\frac{1}{n_{\rm b}}\frac{1}{r^2}\frac{\partial}{\partial r}r^2 n_{\rm b}\xi^0_{\rm br} + \frac{\partial}{\partial\theta}\sin\theta\xi^0_{{\rm b}\theta} + \imath m\xi^0_{{\rm b}\phi} = 0, \tag{11}$$

$$\frac{1}{n_{\rm e}}\frac{1}{r^2}\frac{\partial}{\partial r}r^2 n_{\rm e}\left(\xi^0_{\rm br} - z^0_r\right) + \frac{\partial}{\partial\theta}\sin\theta\left(\xi^0_{{\rm b}\theta} - z^0_\theta\right) + \imath m\left(\xi^0_{{\rm b}\phi} - z^0_\phi\right) = 0, \tag{12}$$

$$-\sigma_0^2 z^0_r - 2\imath\frac{h_1}{h}\sigma_0\sin\theta z^0_\phi = -\frac{c^2 n_{\rm e}}{h}\frac{\partial}{\partial r}\Delta\mu_{\rm e}^1, \tag{13}$$

$$-\sigma_0 z^0_\theta - 2\imath\frac{h_1}{h}\cos\theta z^0_\phi = -\frac{1}{\imath m}\frac{\partial}{\partial\theta}\sin\theta\left[\sigma_0 z^0_\phi - 2\imath\frac{h_1}{h}\left(z^0_r\sin\theta + z^0_\theta\cos\theta\right)\right], \tag{14}$$

$$-\sigma_0^2 z^0_\phi + 2\imath\frac{h_1}{h}\sigma_0\left(z^0_r\sin\theta + z^0_\theta\cos\theta\right) = -\frac{c^2 n_{\rm e}}{h}\frac{\imath m}{r\sin\theta}\Delta\mu_{\rm e}^1. \tag{15}$$

Here we (i) substituted (5)–(7) into equations (1)–(3), (ii) omitted higher-order in Ω/Ω_0 terms, (iii) substituted δP^1 from ϕ-component of Euler equation (10) into the θ-component of Euler equation, (iv) substituted $\Delta\mu_{\rm e}^1$ from ϕ-component of superfluid equation (15) into the θ-component of superfluid equation, (v) expressed in (8) δw through δP and $\Delta\mu_{\rm e}$ (see Kantor & Gusakov 2017, Appendix A), and (vi) divided superfluid equation by $-h(r)$.

It is convenient to express the functions $\xi^0_{{\rm b}\theta}$, $\xi^0_{{\rm b}\phi}$, z^0_θ, and z^0_ϕ in the system (8)–(15) as a sum of toroidal and poloidal

[1] We assume that all non-superfluid components (electrons as well as non-superfluid neutrons and protons) move with the same velocity, due to efficient particle collisions

components (Saio 1982):

$$\xi^0_{\mathrm{b}\theta} = \frac{\partial}{\partial\theta}Q(r,\theta) + \frac{\imath m T(r,\theta)}{\sin\theta}, \quad \xi^0_{\mathrm{b}\phi} = \frac{\imath m Q(r,\theta)}{\sin\theta} - \frac{\partial}{\partial\theta}T(r,\theta), \tag{16}$$

$$z^0_\theta = \frac{\partial}{\partial\theta}Q_z(r,\theta) + \frac{\imath m T_z(r,\theta)}{\sin\theta}, \quad z^0_\phi = \frac{\imath m Q_z(r,\theta)}{\sin\theta} - \frac{\partial}{\partial\theta}T_z(r,\theta). \tag{17}$$

Then, following the same procedure as for non-superfluid stars (e.g., Lockitch & Friedman 1999), we expand all the unknown functions into Legendre polynomial series with fixed m:

$$\xi^0_{\mathrm{br}}(r,\theta) = \sum_{l_2} \xi^0_{\mathrm{br}\,l_2 m}(r) P^m_{l_2}(\cos\theta), \tag{18}$$

$$z_r(r,\theta) = \sum_{l_2} z^0_{r\,l_2 m}(r) P^m_{l_2}(\cos\theta), \tag{19}$$

$$Q(r,\theta) = \sum_{l_2} Q_{l_2 m}(r) P^m_{l_2}(\cos\theta), \tag{20}$$

$$Q_z(r,\theta) = \sum_{l_2} Q_{z\,l_2 m}(r) P^m_{l_2}(\cos\theta), \tag{21}$$

$$T(r,\theta) = \sum_{l_1} T_{l_1 m}(r) P^m_{l_1}(\cos\theta), \tag{22}$$

$$T_z(r,\theta) = \sum_{l_1} T_{z\,l_1 m}(r) P^m_{l_1}(\cos\theta), \tag{23}$$

$$\delta P^1(r,\theta) = \sum_{l_2} \delta P^1_{l_2 m}(r) P^m_{l_2}(\cos\theta), \tag{24}$$

$$\Delta\mu^1_{\mathrm{e}}(r,\theta) = \sum_{l_2} \Delta\mu^1_{\mathrm{e}\,l_2 m}(r) P^m_{l_2}(\cos\theta), \tag{25}$$

where the summation goes over $l_1 = m + 2k$ and $l_2 = m + 2k + 1$ ($k = 0, 1, 2, \ldots$) for 'odd' modes, and over $l_1 = m + 2k + 1$, $l_2 = m + 2k + 2$ for 'even' modes.[2] After substituting these expansions into oscillation equations, one obtains an infinite set of ordinary differential equations for unknown functions $\xi^1_{\mathrm{br}\,l_2 m}(r)$, $z^1_{r\,l_2 m}(r)$, ...

3 CLASSIFICATION OF ROTATIONAL MODES

We are considering rotational modes, with $\sigma \propto \Omega$ at slow rotation limit (Lockitch & Friedman 1999; Yoshida & Lee 2000). Each mode is characterized by two angular quantum numbers, l_0 and m, where m is azimuthal number and l_0 (in the notation by Lindblom & Ipser 1999; Yoshida & Lee 2000) is the maximum index l of spherical harmonics associated with the dominant expansion coefficients of the eigenfunctions. For the uniform density stars all coefficients with $l > l_0$ are strictly zero (Lockitch & Friedman 1999).

For a given m, there are two nodeless modes with $l_0 - |m| = 1$: the (purely toroidal) normal r-mode with $\sigma_0 = 2/(m+1)$, and the superfluid r-mode, which in the limit $Y_{\mathrm{np}} = 0$ is also purely toroidal and has the same frequency (Andersson & Comer 2001; Lee & Yoshida 2003; Andersson et al. 2009; Kantor & Gusakov 2017). For a given m and $l_0 > |m| + 1$ there are $l_0 - |m|$ normal inertial modes (i^0-modes) and $l_0 - |m|$ superfluid inertial modes (i^s-modes). The modes where normal and superfluid components are comoving, so that $|\boldsymbol{\xi}_{\mathrm{b}}| \sim |\boldsymbol{z}|$, we call 'normal' and denote them with superscript ^{0}; If normal and superfluid components are counter-moving, so that the total baryon current is almost not excited, $|\boldsymbol{\xi}_{\mathrm{b}}| \ll |\boldsymbol{z}|$, the corresponding modes are referred to as 'superfluid', and have superscript ^{s}. The number of radial nodes in eigenfunctions of a given mode is determined by l_0 and m (see Yoshida & Lee 2000, Table 3). For example, the dominant lowest-order toroidal eigenfunction [$T_{mm}(r)$ for i^0-modes, $T_{z\,mm}(r)$ for i^s-modes] has zero nodes for the r-mode ($l_0 - |m| = 1$), one node for $l_0 - |m| = 3$ mode, and two nodes for $l_0 - |m| = 5$ mode.

4 RESULTS FOR THE SPECTRUM

For the calculations we adopt the parametrization Heiselberg & Hjorth-Jensen (1999) of APR equation of state (Akmal et al. 1998) for the *npe* matter in the core, and the equation of state BSk20 Potekhin et al. (2013) to describe the crust. All calculations are performed for a NS with mass $M = 1.4 M_\odot$ and radius $R = 12.18$ km. We also assume that baryon critical temperatures are constant throughout the core: $T_{\mathrm{cn}} = 6 \times 10^8$ K, $T_{\mathrm{cp}} = 5 \times 10^9$ K (except for Fig. 2, where we set

[2] Following Yoshida & Lee (2000), we call 'even' the modes whose scalar perturbations are symmetric with respect to the equator, and 'odd' – the modes with asymmetric perturbations. Odd and even modes are completely decoupled and do mix with each other.

$T_{\rm cn} = 5 \times 10^9$ K, $T_{\rm cp} = 5 \times 10^8$ K). The entrainment matrix $Y_{\rm ik}$ is calculated in a way similar to how it was done in Kantor & Gusakov (2011).

They key ingredients of the scenario proposed by Gusakov et al. (2014a,b) are the avoided crossings of inertial modes with the $m = 2$ normal r-mode. We calculated only the modes that could interact with this mode, i.e. the odd ($l_0 - |m| = 1$, $l_0 - |m| = 3$, and $l_0 - |m| = 5$) $m = 2$ inertial modes. We do not look for the modes with eigenfrequencies that are too far from the r-mode frequency ($\sigma_0 = 2/(m+1) = 2/3$). In order to solve the oscillation equations (8)–(15) numerically, we disregard all the terms with $l > |m| + 2k_{\rm max} - 1$ in the Legendre polynomial expansion. We set $k_{\rm max} = 3$ to calculate $l_0 - |m| = 3$ and $l_0 - |m| = 5$ modes. This value allows to reproduce the results of Yoshida & Lee (2000) for the $l_0 - |m| = 3$ inertial modes within the accuracy of 0.2%. For r-modes ($l_0 - |m| = 1$), for which only $l = m$ and $l = m + 1$ harmonics are significant, we set $k_{\rm max} = 2$.

In Fig. 1 we show the spectrum for $l_0 - |m| = 1$, $l_0 - |m| = 3$, and $l_0 - |m| = 5$ inertial modes. Dashed lines denote the i-modes calculated without entrainment ($Y_{\rm np} = 0$), solid lines – with entrainment. The blue line is the normal $m = 2$ r^0-mode, $\sigma_0 = 2/3$ (note that if $Y_{\rm np} = 0$ the superfluid r-mode has the same frequency in the lowest order in Ω, see Andersson & Comer 2001; Lee & Yoshida 2003; Andersson et al. 2009; Kantor & Gusakov 2017). The dot-dashed line denotes the superfluid r-mode calculated analytically via the approximate method described in Sec. 5. This approximate method accounts for the first-order terms in $\Delta h \equiv h_1/h - 1$ and thus its accuracy can be estimated as Δh^2. In Fig. 6 we plot the ratio $h_1(r)/h(r)$ for our NS model at $T = 10^7$ K (dashed line) and $T = 5.5 \times 10^8$ K (dot-dashed line). As one can see from this Figure, Δh at low temperatures is much larger than at temperatures close to $T_{\rm cn}$: $\Delta h \gtrsim 0.2$ at $T = 10^7$ K, $\Delta h \lesssim 0.02$ at $T = 5.5 \times 10^8$ K. Therefore one can expect that at $T \to T_{\rm cn}$ the r^s-mode frequency will approach the value $\sigma_0 = 2/(m+1)$, and the analytical method accuracy will increase. Indeed, we observe it in Fig. 1. One can see that even at low temperatures, when the frequency of r^s-mode significantly differs from the normal r^0-mode, the two methods of calculating the frequency of r^s-mode give the same result within the accuracy of 1%. For example, at $T = 10^7$ K numerical calculation for r^s-mode yields $\sigma_0 = 0.8452$, while the analytical result is $\sigma_0 = 0.8476$. At higher temperatures $T > 3 \times 10^8$ K the relative difference numerical and analytical results does not exceed 0.01%. Note, however, that the approximate method does not provide such great accuracy for eigenfunctions calculation (see discussion of Fig. 5 below).

The spectrum of inertial modes exhibits some interesting features: (i) At low temperatures in the absence of entrainment the frequencies of the normal and superfluid i-modes almost coincide. (ii) While the entrainment effect almost does not affect the normal inertial modes (i^0-modes), it noticeably pushes the frequencies of superfluid modes up. We discuss this behavior in Sec. 6. In order to illustrate the transition from the case $Y_{\rm np} \neq 0$ to $Y_{\rm np} = 0$, we show on Fig. 2 the spectrum for the same modes, but employing another (non-realistic) critical temperatures: $T_{\rm cp} = 5 \times 10^8$ K, $T_{\rm cn} = 5 \times 10^9$ K. The absolute value of $Y_{\rm np}$ decreases as the temperature goes up, and turns into zero at $T = T_{\rm cp}$, when all protons become non-superconducting. (iii) In contrast to the normal r^0-mode, which has the same frequency in the whole temperature range in both superfluid and non-superfluid NSs, the frequencies of the normal i^0-modes at temperatures close to $T_{\rm cn}$ do not remain constant but go down. This is not surprising, since non-superfluid stratified *npe*-matter of NS cores does not support inertial modes. Superfluid i^s-mode frequencies, in contrast, grow at $T \to T_{\rm cn}$. In order to explain all these features, in Sec. 6 we analyze a dispersion relation for inertial modes in short-wavelength limit (see Eqs. 71-75 and their discussion).

In Fig. 1 one can see avoided crossings of the $l_0 - |m| = 3$ normal i^0-mode and its neighbouring $l_0 - |m| = 5$ superfluid i^s-mode (see red lines) at $T \sim 10^8$ K and at $T \sim 5.5 \times 10^8$ K: normal mode transforms into superfluid, and vice versa. We did not find any avoided crossing between superfluid i^s-modes and the normal r^0-mode, and, thus, the stability peaks for the scenario proposed by Gusakov et al. (2014a,b). However, there should be an interaction between normal and superfluid r-modes at $T \to T_{\rm cn}$, which can stabilize normal r^0-mode, and result in the formation of the stability peak at $T = T_{\rm cn}$. Notice also that at low temperatures the frequency of $l_0 - |m| = 3$ superfluid i^s-mode is rather close to the frequency of the normal r^0-mode this may also lead to the stabilizing interaction of modes at low temperatures. One has to take into account the next-order terms in Ω to work out these interactions, which is out of scope of this paper. Here we considered only one particular simplified model and modes with low l_0. One may expect to find avoided-crossings of r^0-modes under more realistic physical assumptions. Further we are going to calculate the spectrum using realistic critical temperature profiles and accounting for muons, which play very important role in defining oscillation spectrum (Kantor & Gusakov 2017).

In order to illustrate properties of inertial modes, we also plot their eigenfunctions. Fig. 3 shows eigenfunctions for $2 \leq l \leq 7$ harmonics of toroidal, poloidal and radial displacements for $l_0 - |m| = 3$ i^0-mode at $T = 10^7$ K. One can see that the baryon displacements (blue lines) are significantly larger than the superfluid ones (red lines). The each of the dominant eigenfunctions $T_{22}(r)$, Q_{32} and $\xi_{{\rm b}r\,32}$ has one radial node,[3] in accordance with Table 3 in the paper by Yoshida & Lee (2000).

The lowest harmonics for $l_0 - |m| = 3$ and $l_0 - |m| = 5$ normal and superfluid i-modes are plotted in Fig. 4. Eigenfunctions are normalized so that $\imath T_{22}(R_{cc}) = 1$ for i^0-modes, and $\imath T_{z\,22}(R_{cc}) = 1$ for i^s-modes. One can clearly see the key difference between the normal and superfluid modes: for normal modes (top left and top right panel) baryon displacements (blue lines)

[3] Following Yoshida & Lee (2000), we include the node at the stellar surface in the count of nodes.

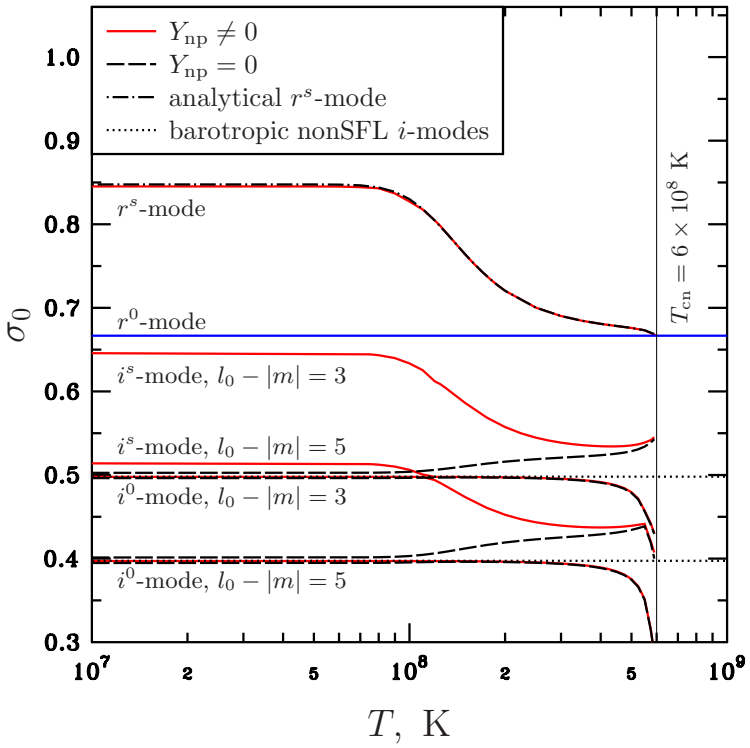

Figure 1. Eigenfrequency σ_0 versus stellar temperature T for $m = 2$ inertial modes. Critical temperatures are constant throughout the core, $T_{\rm cn} = 6 \times 10^8$ K, $T_{\rm cp} = 5 \times 10^9$ K. Solid lines denote inertial modes calculated with taking into account the entrainment effect ($Y_{\rm np} \neq 0$), dashed lines denote the same modes calculated without the entrainment effect. Dot-dashed line denotes the superfluid r^s-mode calculated via the approximate analytical method introduced in Sec. 5. Dotted lines correspond to $l_0 - |m| = 3$ and $l_0 - |m| = 5$ normal i-modes in a non-superlfuid barotropic NS with the same EOS and mass. In all cases the $m = 2$ normal r-mode (blue line) has the same frequency $\sigma_0 = 2/3$.

are comparable (and even larger) with the superfluid ones (red lines), while for superfluid modes (bottom left and bottom right panel) superfluid displacements dominate. It is also interesting that toroidal displacements are larger than poloidal for all considered modes. The lowest-order dominant eigenfunctions ($T_{22}(r)$, Q_{32} and $\xi_{{\rm br}\,32}$ for i^0-modes, $T_{z\,22}(r)$, $Q_{z\,32}$ and $z_{r\,32}$ for i^s-modes) have one radial node for the case $l_0 - |m| = 3$ (left) and two nodes $l_0 - |m| = 5$ – again, as expected from Table 3 in the paper by Yoshida & Lee (2000). Note that, e.g. $T_{22}(r)$ for the $l_0 - |m| = 3$ i^s-mode has more nodes than $T_{z\,22}(r)$ and cannot be used for determining the value of l_0.

We also compare eigenfunctions obtained via numerical calculations and via analytical method from Sec. 5 for the superfluid r^s-mode at low ($T = 10^7$ K) and high ($T = 5.5 \times 10^8$ K) temperatures. The results are shown in Fig. 5. Solid lines represent the numerical results, and dashed lines show analytical results. For $T = 10^7$ K (left panel) we plotted only the superfluid displacements $T_{z\,22}(r)$, $Q_{z\,32}$ and $z_{r\,32}$ because they are much larger than the baryon ones. Since the toroidal component is dominating, we multiplied $Q_{z\,32}$ and $z_{r\,32}$ by 10 in order to make them visible. We see that both method lead to qualitatively similar, bu quantitatively different result: while the eigenfrequencies coincide within the accuracy of 1%, eigenfunctions differs significantly. At $T = 5.5 \times 10^8$ K (right panel), where entrainment effect is small (see Fig. 6) and the r^s-mode frequency is close to that of r^0-mode, analytical method becomes more accurate. Indeed, we see that in this case the eigenfunctions coincide much better, within the accuracy of 10%. Here we plotted the superfluid and baryon toroidal displacements, $T_{z\,22}(r)$ and $T_{22}(r)$, since at this temperature they are much larger than all other eigenfunctions. The large value of $T_{22}(r)$ indicates a possible interaction with the normal r-mode. From the analysis of Figs 1, 2 and 5 we conclude that the approximate method of calculating the superfluid r-mode gives a very good accuracy (better than 1%) for eigenfrequencies, but one has to keep in mind that the eigenfunctions are calculated much less accurately, especially when entrainment effect is large (e.g. at low temperatures).

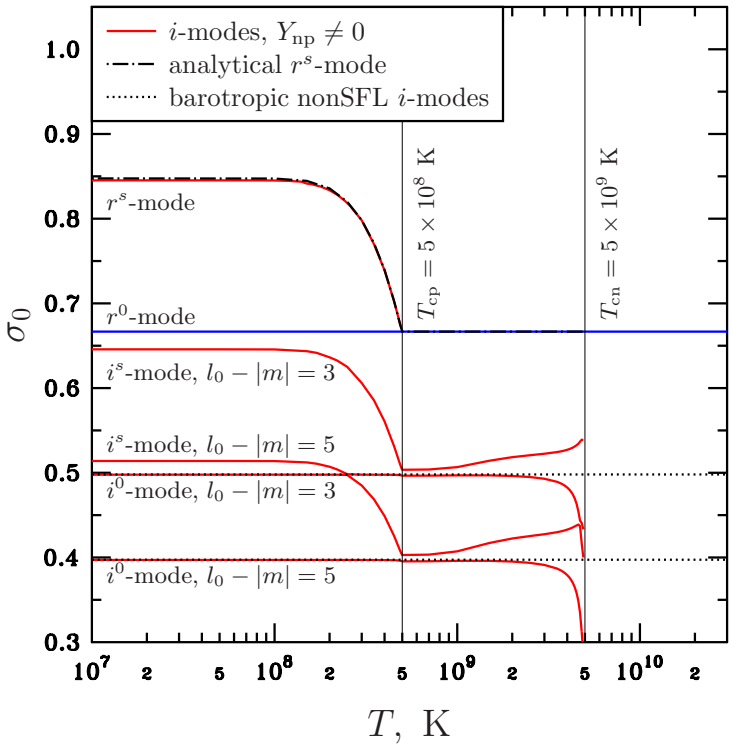

Figure 2. Eigenfrequency σ_0 versus stellar temperature T for $m = 2$ inertial modes. Critical temperatures are constant throughout the core, $T_{\rm cn} = 5 \times 10^9$ K, $T_{\rm cp} = 5 \times 10^8$ K. Solid lines denote inertial modes calculated with taking into account the entrainment effect ($Y_{\rm np} \neq 0$ at $T < T_{\rm cp}$), Dot-dashed line denotes the superfluid r^s-mode calculated via the approximate analytical method introduced in Sec. 5. Dotted lines correspond to $l_0 - |m| = 3$ and $l_0 - |m| = 5$ normal i-modes in a non-superlfuid barotropic NS with the same EOS and mass. In all cases the $m = 2$ normal r-mode (blue line) has the same frequency $\sigma_0 = 2/3$.

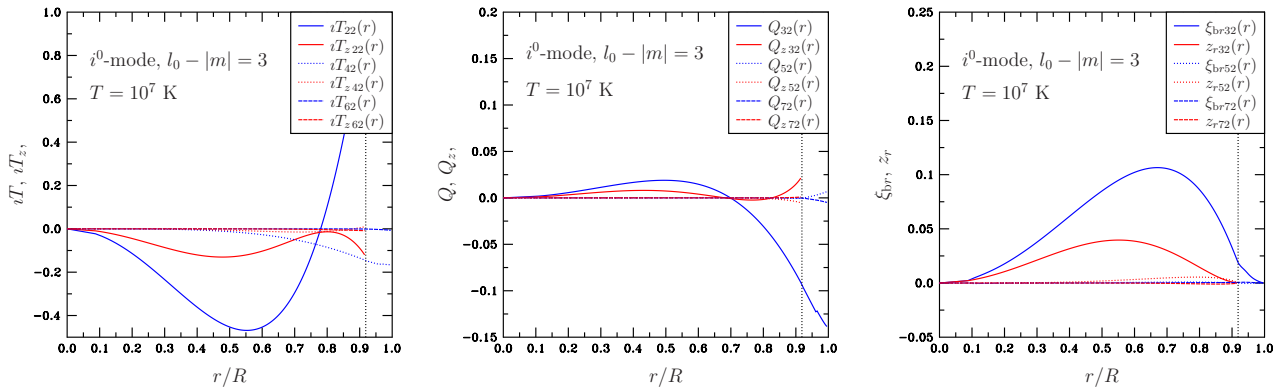

Figure 3. The lowest three harmonics for toroidal (left panel), poloidal (central panel) and radial (right panel) displacements for the $m = 2$, $l_0 - |m| = 3$ normal i^0-mode at $T = 10^7$ K. Blue lines denotes Lagrangian displacements for baryons, and red lines denotes superfluid displacements. Critical temperatures are constant throughout the core, $T_{\rm cn} = 6 \times 10^8$ K, $T_{\rm cp} = 5 \times 10^9$ K. Vertical dots show the crust-core interface.

5 SUPERFLUID R-MODE IN THE LIMIT OF SMALL ENTRAINMENT

In this section we provide an approximate method that allows one to calculate the superfluid r-mode in *npe* NS analytically in the lowest order in Ω, accounting for entrainment effect. If there is no entrainment ($Y_{\rm np} = 0$), then for a given m there exist two purely toroidal rotational modes, the normal r-mode and the superfluid r-mode, both having (to the lowest order in Ω/Ω_0) the same frequency $\sigma_0 = 2/(m+1)$ (Andersson & Comer 2001; Lee & Yoshida 2003; Andersson et al. 2009; Kantor

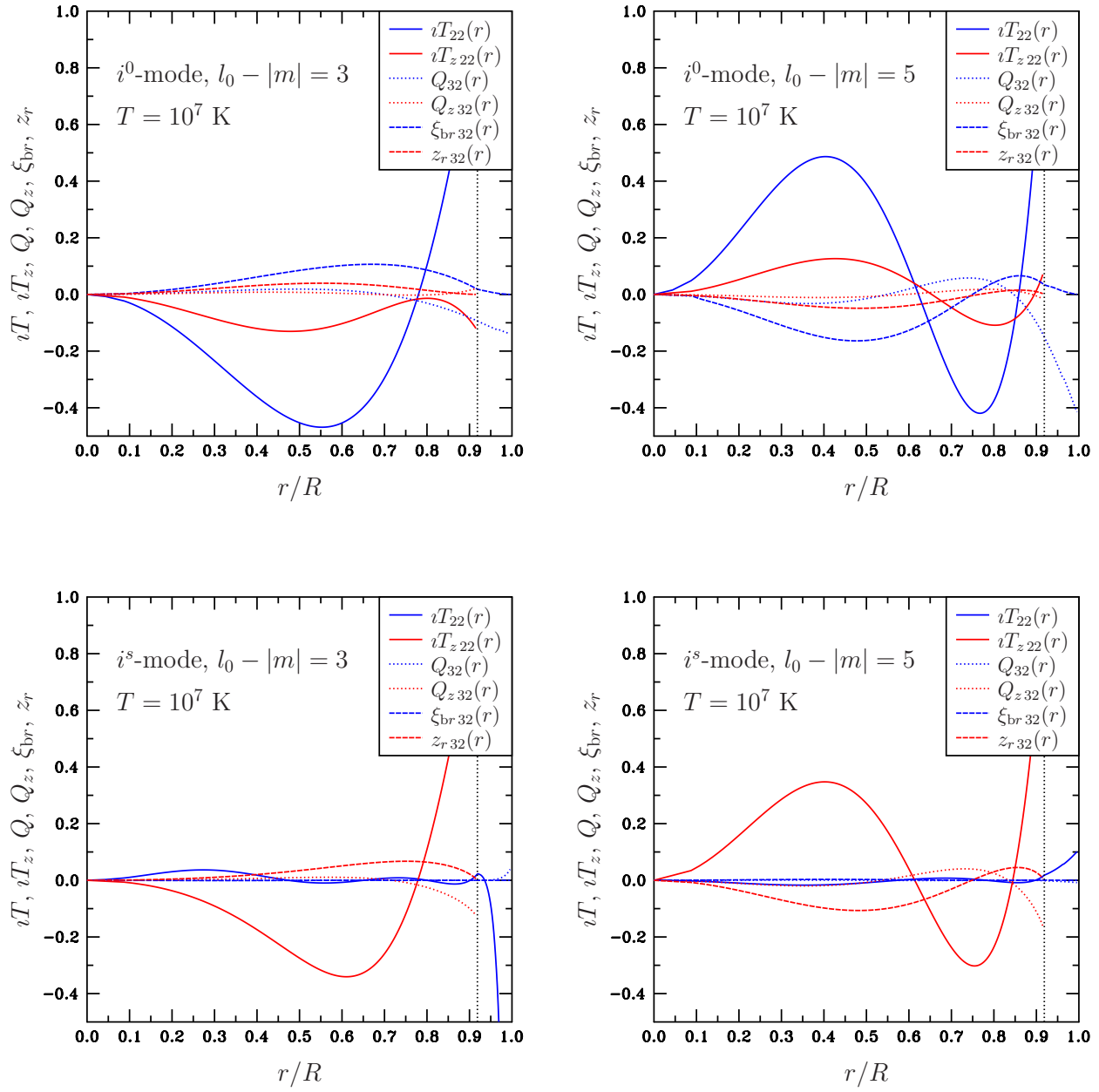

Figure 4. Eigenfunctions for different $m = 2$ inertial modes at $T = 10^7$ K. Top left: $l_0 - |m| = 3$ normal i^0-mode. Top right: $l_0 - |m| = 5$ normal i^0-mode. Bottom left: the $l_0 - |m| = 3$ superfluid i^s-mode. Bottom right: the $l_0 - |m| = 5$ superfluid i^s-mode. Only lowest-order harmonics ($l = 2$ for toroidal displacements T, T_z and $l = 3$ for poloidal and radial displacements Q, Q_z, ξ_{br}, z_r) are plotted. Blue lines denotes Lagrangian displacements for baryons, and red lines denotes superfluid displacements. Critical temperatures are constant throughout the core, $T_{\mathrm{cn}} = 6 \times 10^8$ K, $T_{\mathrm{cp}} = 5 \times 10^9$ K. Vertical dots show the crust-core interface.

& Gusakov 2017). In the case of non-zero entrainment ($Y_{\mathrm{np}} \neq 0$ and thus $h_1 \neq h$, see Eq. 4) the superfluid r-mode turns into a mixed poloidal-toroidal mode with different frequency. Assuming that the entrainment effect is small, one can develop a perturbation theory in $\Delta h \equiv h_1/h - 1$, and find analytically corrections to the eigenfrequency and eigenfunctions for the superfluid r-mode in the first order in Δh. This method is analogous to that of Kantor & Gusakov (2017), who showed that in *npe* matter r-modes can be calculated analytically in the next-to-leading order in Ω, but ignoring the entrainment effect (i.e assuming $h_1 = h$).

Let us start with purely toroidal oscillations, for which radial displacements vanish ($\xi_{\mathrm{br}} = z_r = 0$). The continuity

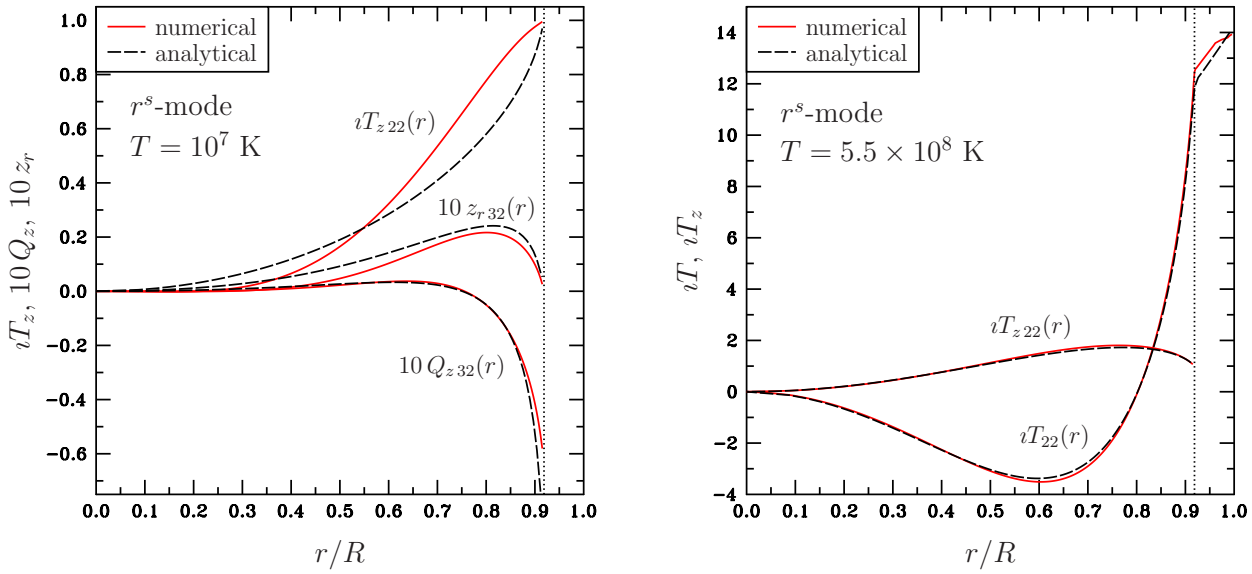

Figure 5. Dominant eigenfunctions for the $m = 2$ superfluid r-mode, obtained by numerical calculations (solid lines) and by the approximate analytical method (dashed lines). Left panel displays superfluid displacements $T_{z\,22}$, $Q_{z\,32}$ (multiplied by 10), and $Q_{z\,32}$ (multiplied by 10) for $T = 10^7$ K. Right panel displays toroidal displacements $T_{z\,22}$ and T_{22} for $T = 5.5 \times 10^8$ K. Critical temperatures are constant throughout the core, $T_{\rm cn} = 6 \times 10^8$ K, $T_{\rm cp} = 5 \times 10^9$ K. Vertical dots show the crust-core interface.

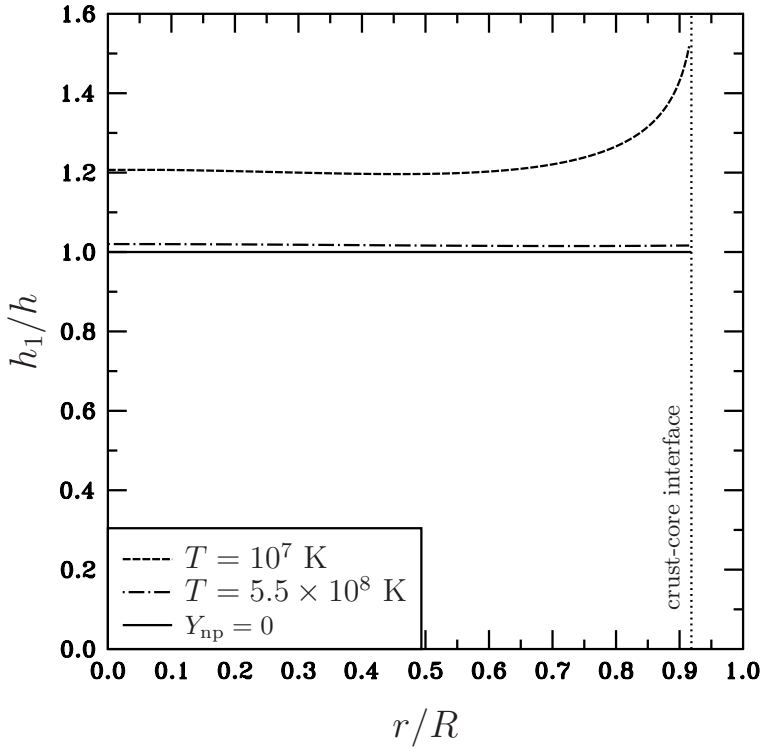

Figure 6. The ratio h_1/h versus normalized radial coordinate r/R for temperatures $T = 10^7$ K (dashed line) and $T = 5.5 \times 10^8$ K (dot-dashed line). Critical temperatures are constant throughout the core, $T_{\rm cn} = 6 \times 10^8$ K, $T_{\rm cp} = 5 \times 10^9$ K. In the absence of entrainment ($Y_{\rm np} = 0$) $h_1/h \equiv 1$ (solid line).

equations (11) and (12) in this case reduce to

$$\frac{\partial}{\partial\theta}\sin\theta\xi^0_{\mathrm{b}\theta}+\imath m\xi^0_{\mathrm{b}\phi}=0, \tag{26}$$

$$\frac{\partial}{\partial\theta}\sin\theta z^0_{\theta}+\imath m z^0_{\phi}=0. \tag{27}$$

θ-components of Euler equation (9) and superfluid equation (14) read

$$-\sigma_0\xi^0_{\mathrm{b}\theta}-2\imath\cos\theta\xi^0_{\mathrm{b}\phi}=\frac{1}{\imath m}\frac{\partial}{\partial\theta}\sin\theta\left(-\sigma_0\xi^0_{\mathrm{b}\phi}+2\imath\xi^0_{\mathrm{b}\theta}\cos\theta\right), \tag{28}$$

$$-\sigma_0 z^0_{\theta}-2\imath\frac{h_1}{h}\cos\theta z^0_{\phi}=-\frac{1}{\imath m}\frac{\partial}{\partial\theta}\sin\theta\left(\sigma_0 z^0_{\phi}-2\imath\frac{h_1}{h}z^0_{\theta}\cos\theta\right). \tag{29}$$

The solution to the system of equations (26) and (28) is

$$\sigma_0=\frac{2m}{l(l+1)},\quad \xi^0_{\mathrm{b}\theta}=\frac{\imath m}{\sin\theta}T_{lm}(r)P^m_l(\cos\theta),\quad \xi^0_{\mathrm{b}\phi}=-T_{lm}(r)\frac{d}{d\theta}P^m_l(\cos\theta), \tag{30}$$

which is the well-known normal r-mode. One can check that only the solution with $l=m$ satisfies equations (8) and (10).

The second pair of equations, (27) and (29), describe the superfluid r-mode,

$$\sigma_0=\frac{2m}{l(l+1)}\frac{h_1(r)}{h(r)},\quad z^0_{\theta}=\frac{\imath m}{\sin\theta}T_{z\,lm}(r)P^m_l(\cos\theta),\quad z^0_{\phi}=-T_{z\,lm}(r)\frac{d}{d\theta}P^m_l(\cos\theta). \tag{31}$$

If $h_1=h$, then $\sigma_0=\frac{2m}{l(l+1)}$ is the global oscillation frequency and the superfluid r-mode is indeed purely toroidal (and, as for the normal r-mode, only $l=m$ solution exist). However, if the entrainment effect is present, $h_1(r)/h(r)$ in general case varies throughout the star. This means that the purely toroidal superfluid mode cannot exist, and an admixture of poloidal component is required.

Now let us write a perturbation theory in $\Delta h\equiv h_1/h-1$. Below we denote the zeroth-order in Δh quantities with index (0), and the first-order in Δh quantities – with index (1).

In this notation, the eigenfrequency σ_0 and eigenfunctions can be written in series in Δh as

$$\sigma_0=\sigma_{0(0)}+\sigma_{0(1)}+O(\Delta h^2)=\frac{2}{m+1}+\sigma_{0(1)}+O(\Delta h^2), \tag{32}$$

$$\xi^0_{\mathrm{br}}=\xi^{0(1)}_{\mathrm{br}}+O(\Delta h^2),\quad T=T^{(0)}+T^{(1)}+O(\Delta h^2),\quad Q=Q^{(1)}+O(\Delta h^2), \tag{33}$$

$$z^0_r=z^{0(1)}_r+O(\Delta h^2),\quad T_z=T^{(0)}_z+T^{(1)}_z+O(\Delta h^2),\quad Q_z=Q^{(1)}_z+O(\Delta h^2), \tag{34}$$

$$\delta P=\delta P^{1(0)}+\delta P^{1(1)}+O(\Delta h^2), \tag{35}$$

$$\Delta\mu^1_{\mathrm{e}}=\Delta\mu^{1(0)}_{\mathrm{e}}+\Delta\mu^{1(1)}_{\mathrm{e}}+O(\Delta h^2). \tag{36}$$

Since in absence of entrainment the superfluid r-mode is purely toroidal, radial and poloidal displacements in the zeroth order vanish, $\xi^{0(0)}_{\mathrm{br}}=z^{0(0)}_r=Q^{(0)}=Q^{(0)}_z=0$.

5.1 Zero-order solution

In zeroth order in Δh (i.e. without the entrainment effect) one has to find the eigenfrequency $\sigma_{0(0)}$ and four eigenfunctions $T^{(0)},T^{(0)}_z,\delta P^{1(0)},\Delta\mu^{1(0)}_{\mathrm{e}}$. As discussed above (see Eqs. 30 and 31), the frequency equals to

$$\sigma_{0(0)}=\frac{2}{m+1}, \tag{37}$$

and the toroidal displacements are proportional to the $l=m$ Legendre polynomial,

$$T^{(0)}=T^{(0)}_{mm}(r)P^m_m(\cos\theta),\quad T^{(0)}_z=T^{(0)}_{zmm}(r)P^m_m(\cos\theta). \tag{38}$$

One can obtain from Eqs. (8), (10), (13), and (15) that the perturbations $\delta P^{1(0)}$ and $\Delta\mu^{1(0)}_{\mathrm{e}}$ are proportional to the $l=m+1$ Legendre polynomial,

$$\delta P^{1(0)}=\delta P^{1(0)}_{m+1,m}(r)P^m_{m+1}(\cos\theta),\quad \Delta\mu^{1(0)}_{\mathrm{e}}=\Delta\mu^{1(0)}_{\mathrm{e}\,m+1,m}(r)P^m_{m+1}(\cos\theta), \tag{39}$$

while the coefficients $\delta P^{1(0)}_{m+1,m}(r)$, $\Delta\mu^{1(0)}_{\mathrm{e}\,m+1,m}(r)$ are expressed through $T^{(0)}_{mm}(r)$ and $T^{(0)}_{zmm}(r)$ respectively:

$$\delta P^{1(0)}_{m+1,m}(r)=\frac{\imath\sigma_{0(0)}(\sigma_{0(0)}-2)}{2m+1}w_0T^{(0)}_{mm}(r), \tag{40}$$

$$\Delta\mu^{1(0)}_{\mathrm{e}\,m+1,m}(r)=\frac{\imath\sigma_{0(0)}(\sigma_{0(0)}-2)}{2m+1}\frac{h}{c^2n_{\mathrm{e}}}T^{(0)}_{zmm}(r). \tag{41}$$

After substituting the expressions for $\Delta\mu^{1(0)}_{\mathrm{e}}$ and $\delta P^{1(0)}$ into Eqs. (13) and (8), one can finally obtain the solution for

$T^{(0)}_{zmm}(r)$ and $T^{(0)}_{mm}(r)$ (see Kantor & Gusakov 2017, Appendix B),

$$T^{(0)}_{zmm}(r) = C_1 \frac{n_\mathrm{e}(r)}{h(r)} r^m, \tag{42}$$

$$T^{(0)}_{mm}(r) = r^m \left(C_0 + C_1 \int_0^r \frac{\mu_\mathrm{n}(r_1)}{c^4 w_0(r_1)} \frac{dP_0(r_1)}{dr_1} \frac{\partial n_\mathrm{b}}{\partial \Delta\mu_\mathrm{e}}(r_1) \mathrm{d}r_1 \right). \tag{43}$$

The integration constants C_0 and C_1 have to be determined from the first-order equations.

5.2 First-order solution

To find the eigenfrequency correction $\sigma_{0(1)}$ and the constants C_0 and C_1, it is sufficient to consider only continuity equations (11)–(12) as well as θ-components of the Euler equation (9) and the superfluid equation (14).

θ-component of the Euler equation in first order in Δh [i.e. ignoring quadratically small terms like $\sigma_{0(1)}\xi^{0(1)}_{\mathrm{b}\theta}$] reads

$$-\sigma_{0(1)}\xi^{0(0)}_{\mathrm{b}\theta} - \sigma_{0(0)}\xi^{0(1)}_{\mathrm{b}\theta} - 2\imath\cos\theta\,\xi^{0(1)}_{\mathrm{b}\phi} = \frac{1}{\imath m}\frac{\partial}{\partial\theta}\sin\theta\left[-\sigma_{0(1)}\xi^{0(0)}_{\mathrm{b}\phi} - \sigma_{0(0)}\xi^{0(1)}_{\mathrm{b}\phi} + 2\imath\left(\xi^{0(1)}_{\mathrm{br}}\sin\theta + \xi^{0(1)}_{\mathrm{b}\theta}\cos\theta\right)\right]. \tag{44}$$

Substituting relations (16), (18), (20), (22) into Eq. (44) divided by $\sin\theta$ and equating coefficients at the terms proportional to P^m_m, one can express $Q^{(1)}_{m+1,m}(r)$ through $\xi^{0(1)}_{\mathrm{br}\,m+1,m}(r)$ and $T^{(0)}_{mm}(r)$.

Similarly, using θ-component of the superfluid equation

$$-\sigma_{0(1)}z^{0(0)}_\theta - \sigma_{0(0)}z^{0(1)}_\theta - 2\imath\Delta h\cos\theta z^{0(0)}_\phi - 2\cos\theta z^{0(1)}_\phi = -\frac{1}{\imath m}\frac{\partial}{\partial\theta}\sin\theta\left[\sigma_0 z^{0(1)}_\phi - 2\imath\left(z^{0(1)}_r\sin\theta + z^{0(1)}_\theta\cos\theta\right) - 2\imath\Delta h z^{0(0)}_\theta\cos\theta\right], \tag{45}$$

one can obtain an algebraic relation between $Q^{(1)}_{z\,m+1,m}(r)$, $z^{0(1)}_{r\,m+1,m}(r)$ and $T^{(0)}_{z\,mm}(r)$.

Now, taking the coefficient at P^m_{m+1} in the continuity equation for baryons

$$\frac{1}{n_\mathrm{b}}\frac{1}{r^2}\frac{\partial}{\partial r}r^2 n_\mathrm{b}\xi^{0(1)}_{\mathrm{br}} + \frac{1}{r\sin\theta}\left[\frac{\partial}{\partial\theta}\sin\theta\frac{\partial Q^{(1)}}{\partial\theta} - \frac{m^2 Q^{(1)}}{\sin\theta}\right] = 0, \tag{46}$$

expressing $Q^{(1)}_{m+1,m}$ through $T^{(0)}_{mm}$ and $\xi^{0(1)}_{\mathrm{br},m+1,m}$, and substituting expression for $T^{(0)}_{mm}$ (43), we get a first-order inhomogeneous ODE for $\xi_{\mathrm{br},m+1,m}$:

$$\frac{d}{dr}\xi^{0(1)}_{\mathrm{br},m+1,m} + A(r)\xi^{0(1)}_{\mathrm{br},m+1,m} + \sigma_{0(1)}C_0 B_{10}(r) + \sigma_{0(1)}C_1 B_{11}(r) = 0, \tag{47}$$

where $A(r), B_{10}(r), B_{11}(r)$ are known functions of r. The solution to this equation is

$$\xi^{0(1)}_{\mathrm{br},m+1,m}(r) = H(r)\left[\xi_0 + \sigma_{0(1)}C_0\int_0^r \frac{B_{10}(x)}{H(x)}\mathrm{d}x + \sigma_{0(1)}C_1\int_0^r\frac{B_{11}(x)}{H(x)}\mathrm{d}x\right], \quad H(r) \equiv \exp\left(-\int A(r)\mathrm{d}r\right) = \frac{1}{n_\mathrm{b}(r)r^{m+3}}. \tag{48}$$

Since $\xi^{0(1)}_{\mathrm{br},m+1,m}(r)$ should be finite at $r\to 0$ the integration constant $\xi_0 = 0$.

Following the same procedure for electron continuity equation, we obtain the expression $z^{0(1)}_{r,m+1,m}(r)$,

$$z^{0(1)}_{r,m+1,m}(r) = H_z(r)\left[z_0 + C_1\int_{r_{\mathrm{sfl1}}}^r \frac{B_{z01}(x)}{H_z(x)}\mathrm{d}x + \sigma_{0(1)}C_0\int_{r_{\mathrm{sfl1}}}^r\frac{B_{z10}(x)}{H_z(x)}\mathrm{d}x + \sigma_{0(1)}C_1\int_{r_{\mathrm{sfl1}}}^r\frac{B_{z11}(x)}{H_z(x)}\mathrm{d}x\right], \tag{49}$$

$$H_z(r) \equiv \exp\left(-\int A_z(r)\mathrm{d}r\right) = \frac{1}{n_\mathrm{e}(r)r^{m+3}}, \tag{50}$$

where r_{sfl1} is the inner boundary of superfluid region. If $r_{\mathrm{sfl1}} = 0$, then the integration constant $z_0 = 0$, because z_r should be finite at $r = 0$; otherwise $z_0 = 0$ too because of the boundary condition $z_r = 0$ at the boundary of superfluid region.

The finiteness of ξ_{br} at the stellar surface $r = R$ and vanishing of z_r at the outer superfluid boundary $r = r_{\mathrm{sfl2}}$ imply

$$\sigma_{0(1)}C_0\int_0^R\frac{B_{10}(x)}{H(x)}\mathrm{d}x + \sigma_{0(1)}C_1\int_0^R\frac{B_{11}(x)}{H(x)}\mathrm{d}x = 0, \tag{51}$$

$$C_1\int_{r_{\mathrm{sfl1}}}^{r_{\mathrm{sfl2}}}\frac{B_{z01}(x)}{H_z(x)}\mathrm{d}x + \sigma_{0(1)}C_0\int_{r_{\mathrm{sfl1}}}^{r_{\mathrm{sfl2}}}\frac{B_{z10}(x)}{H_z(x)}\mathrm{d}x + \sigma_{0(1)}C_1\int_{r_{\mathrm{sfl1}}}^{r_{\mathrm{sfl2}}}\frac{B_{z11}(x)}{H_z(x)}\mathrm{d}x = 0. \tag{52}$$

The system (51)–(52) has two independent solutions.[4] The first solution is $\sigma_{0(1)} = C_1 = 0$; it is the normal r-mode,

$$\sigma_0 = \sigma_{0(0)} = \frac{2}{m+1}, \quad T^{(0)}_{mm} = C_0 r^m, \quad T^{(0)}_{zmm} = 0. \tag{53}$$

The second one, having $\sigma_{0(1)} \neq 0$ and $C_1 \neq 0$, is the superfluid r-mode.

We compared this analytical solution with the numerical one (see Section 4) and found that the difference between them does not exceed 1% even at low temperatures, where Δh is relatively large, $\Delta h \sim 0.2 - 0.25$.

[4] The constant C_0 can be set to arbitrary value (e.g. $C_0 = 1$) by choosing an appropriate normalization for eigenfunctions.

The next step is to combine two approximate method and calculate r-modes accounting for both entrainment and next-to-leading-order in Ω terms. Entrainment may significantly shift resonance temperatures, where an avoided crossing of normal and superfluid r-mode occurs, and thus affect the shape of r-mode instability window.

6 WKB ANALYSIS FOR INERTIAL MODES

In this section we obtain a dispersion relation for inertial modes in superfluid *npe* matter, and analyze it in different limiting cases in order to explain behaviour of the modes at low and high temperatures.

Let us find the dispersion relation for inertial modes defined by equations (8)–(15) in a short wavelength limit, where derivatives of any perturbation δA can be replaced as $\frac{\partial}{\partial \boldsymbol{r}}\delta A \to -\imath \boldsymbol{k}\delta A$, where $\boldsymbol{k}$ is the wave vector.

Continuity equation for baryons (11) in this limit reads:

$$-\imath \boldsymbol{k}\boldsymbol{\xi}^0_{\rm b} = 0. \tag{54}$$

Here we omitted the term $\xi^0_{\rm br}{\rm d}(\ln n_{\rm b})/{\rm d}r$ in comparison to $-\imath \boldsymbol{k}\boldsymbol{\xi}^0_{\rm b}$, since the wavelength is assumed to be much smaller than the density scale height, $k^{-1} \ll |{\rm d}\ln n_{\rm b}/{\rm d}r|^{-1}$.

Subtracting continuity equation for electrons (12) from Eq. (11), one obtains

$$-\imath \boldsymbol{k}\boldsymbol{z}^0 - \xi^0_{\rm br}\frac{d\ln x_{\rm e}}{dr} = 0, \quad x_{\rm e} \equiv \frac{n_{\rm e}}{n_{\rm b}}. \tag{55}$$

Euler equation (8)–(10) and superfluid equation (13)–(15) read:

$$-\sigma_0^2\xi^0_{{\rm b}r} - 2\imath\sigma_0\sin\theta\xi^0_{{\rm b}\phi} = \imath k_r\frac{\delta P^1}{w_0} + \frac{\mu_{\rm n}}{w_0^2c^2}\frac{\partial n_{\rm b}}{\partial\Delta\mu_{\rm e}}\Delta\mu_{\rm e}^1\frac{dP_0}{dr}, \tag{56}$$

$$-\sigma_0^2\xi^0_{{\rm b}\theta} - 2\imath\sigma_0\cos\theta\xi^0_{{\rm b}\phi} = \imath k_\theta\frac{\delta P^1}{w_0}, \tag{57}$$

$$-\sigma_0^2\xi^0_{{\rm b}\phi} + 2\imath\sigma_0\left(\xi^0_{{\rm b}r}\sin\theta + \xi^0_{{\rm b}\theta}\cos\theta\right) = \imath k_\phi\frac{\delta P^1}{w_0}, \tag{58}$$

$$-\sigma_0^2 z^0_r - 2\imath\frac{h_1}{h}\sigma_0\sin\theta z^0_\phi = \imath k_r\frac{c^2 n_{\rm e}}{h}\Delta\mu_{\rm e}^1, \tag{59}$$

$$-\sigma_0^2 z^0_\theta - 2\imath\sigma_0\frac{h_1}{h}\cos\theta z^0_\phi = \imath k_\theta\frac{c^2 n_{\rm e}}{h}\Delta\mu_{\rm e}^1, \tag{60}$$

$$-\sigma_0^2 z^0_\phi + 2\imath\frac{h_1}{h}\sigma_0\left(z^0_r\sin\theta + z^0_\theta\cos\theta\right) = \imath k_\phi\frac{c^2 n_{\rm e}}{h}\Delta\mu_{\rm e}^1. \tag{61}$$

Equations (54)–(61) can be written in a form $\mathbf{A}\cdot\boldsymbol{x} = 0$, where $\boldsymbol{x} = \left(\delta P^1, \Delta\mu_{\rm e}^1, \xi^0_{{\rm b}r}, \xi^0_{{\rm b}\theta}, \xi^0_{{\rm b}\phi}, z^0_r, z^0_\theta, z^0_\phi\right)$, and $\mathbf{A}$ is a 8×8 matrix. Dispersion relation between the frequency $\sigma = \sigma_0\Omega$ and the wave vector $\boldsymbol{k}$ can be found by solving the equation $\det\mathbf{A} = 0$, which reduces to a biquadratic equation on σ_0,

$$A\sigma_0^4 + B\sigma_0^2 + C = 0, \tag{62}$$

where the coefficients A, B, C are defined as

$$A = k^4 - \frac{y}{n_{\rm e}^2}\frac{\partial n_{\rm b}}{\partial\Delta\mu_{\rm e}}\frac{dP_0}{dr}\frac{dx_{\rm e}}{dr}\left(k^2 - k_r^2\right), \tag{63}$$

$$B = -4k^2\frac{(\boldsymbol{\Omega k})^2}{\Omega^2}\left[\left(\frac{h_1}{h}\right)^2 + 1\right] + 4\left(\frac{h_1}{h}\right)^2\frac{y}{n_{\rm e}^2}\frac{\partial n_{\rm b}}{\partial\Delta\mu_{\rm e}}\frac{dP_0}{dr}\frac{dx_{\rm e}}{dr}(k^2 - k_r^2), \tag{64}$$

$$C = 16\left(\frac{h_1}{h}\right)^2\frac{(\boldsymbol{\Omega k})^4}{\Omega^4}. \tag{65}$$

To get a further insight into a problem, let us introduce the following quantities: equilibrium speed of sound $c_{\rm eq}$, adiabatic speed of sound $c_{\rm fr}$ and the coupling parameter s, which are defined as

$$c^2_{\rm eq} \equiv c^2\frac{{\rm d}P/{\rm d}r}{\mu_{\rm n}{\rm d}n_{\rm b}/{\rm d}r}, \quad c^2_{\rm fr} \equiv c^2\frac{1}{\mu_{\rm n}}\left(\frac{\partial P}{\partial n_{\rm b}}\right)_{x_{\rm e}}, \quad s \equiv \frac{n_{\rm e}\left(\partial P/\partial n_{\rm e}\right)_{n_{\rm b}}}{n_{\rm b}\left(\partial P/\partial n_{\rm b}\right)_{x_{\rm e}}}. \tag{66}$$

The derivative $\frac{\partial n_{\rm b}}{\partial\Delta\mu_{\rm e}}$ can be expressed in terms of these variables as

$$\left(\frac{\partial n_{\rm b}}{\partial\Delta\mu_{\rm e}}\right)_P = \frac{n_{\rm b}n_{\rm e}}{sw_0}\left(\frac{1}{c^2_{\rm eq}} - \frac{1}{c^2_{\rm fr}}\right). \tag{67}$$

Also, using the hydrostatic equilibrium condition, we express gradients of equilibrium quantities (P_0 and $x_{\rm e0}$) through gravitational acceleration g as

$$\frac{dP_0}{dr} = -w_0 g, \quad \frac{dx_{\rm e}}{dr} = g\frac{x_e}{s}\left(\frac{1}{c^2_{\rm eq}} - \frac{1}{c^2_{\rm fr}}\right). \tag{68}$$

Further, let us introduce the Brunt-Väisälä frequency $\mathcal{N} \equiv g\left(1/c_{\rm eq}^2 - 1/c_{\rm fr}^2\right)^{1/2}$, which enters the dispersion relation for g-modes (Reisenegger & Goldreich 1992), and the 'superfluid' speed $c_{\rm SFL} \equiv sc_{\rm eq}c_{\rm fr}/\sqrt{y(c_{\rm fr}^2 - c_{\rm eq}^2)}$. The latter quantity in the limit $y \to \infty$ (or, equivalently, $T \to T_{\rm cn}$), equals to the superfluid sound speed (see e.g. Andersson & Comer 2001; Gusakov & Andersson 2006).

Using the above definitions, coefficients A and B from Eqs. (63)–(64) can be presented as

$$A = k^4 + \frac{\mathcal{N}^2(k^2 - k_r^2)}{c_{\rm SFL}^2}, \tag{69}$$

$$B = -4k^2\frac{(\boldsymbol{\Omega k})^2}{\Omega^2}\left[\left(\frac{h_1}{h}\right)^2 + 1\right] - 4\frac{\mathcal{N}^2(k^2 - k_r^2)}{c_{\rm SFL}^2}. \tag{70}$$

Now, if we substitute A, B and C into a dispersion relation $\sigma^2 = \Omega^2(-B \pm \sqrt{B^2 - 4AC})/(2A)$, the result will be rather lengthy. To make it more clear, let us note that at low temperatures the ratio $\mathcal{N}/(c_{\rm SFL}k)$ is small, $\mathcal{N}/(c_{\rm SFL}k) \ll 1$. For example, for a wavenumber $k = 10^{-5}$ cm^{-1} and a NS model used in Section 4 at distance from center $r = R/2$ and temperature $T = 10^7$ K this ratio equals $\mathcal{N}/(c_{\rm SFL}k) = 0.013$. [5]

In this limit the dispersion relation has the following form,

$$\sigma^2 = 4\frac{(\boldsymbol{\Omega k})^2}{k^2} - 4\frac{\mathcal{N}^2}{c_{\rm SFL}^2k^2}\frac{(k^2 - k_r^2)}{k^4}\frac{\left(\frac{h_1}{h}\right)^2\Omega^2k^2 - (\boldsymbol{\Omega k})^2}{\left(\frac{h_1}{h}\right)^2 - 1} + O\left(\frac{\mathcal{N}^4}{c_{\rm SFL}^4k^4}\right), \tag{71}$$

$$\sigma^2 = 4\left(\frac{h_1}{h}\right)^2\frac{(\boldsymbol{\Omega k})^2}{k^2} + 4\frac{\mathcal{N}^2}{c_{\rm SFL}^2k^2}\frac{(k^2 - k_r^2)}{k^4}\left(\frac{h_1}{h}\right)^4\frac{\Omega^2k^2 - (\boldsymbol{\Omega k})^2}{\left(\frac{h_1}{h}\right)^2 - 1} + O\left(\frac{\mathcal{N}^4}{c_{\rm SFL}^4k^4}\right). \tag{72}$$

The first relation (71) describes normal i^0-modes. In barotropic matter, where $\mathcal{N} = 0$, they have a standard dispersion relation $\sigma^2 = 4(\boldsymbol{\Omega k})^2/k^2$ (Landau & Lifshitz 1987). The second relation (72) describes superfluid i^s-modes, for which the leading term differs from that of i^0-modes by the factor $(h_1/h)^2$. One can conclude that, as the entrainment effect decreases, frequencies of a given superfluid i^s-mode approaches the frequency of its normal (i^0-mode) counterpart. Indeed, we observe such behaviour for i^s-modes in Fig. 2 at $T < T_{\rm cp}$. Note, however, that the relations (71)–(72) are invalid if there is no entrainment at all ($Y_{\rm np} = 0$ and therefore $h_1 = h$), since they contain terms that are proportional to $\left[(h_1/h)^2 - 1\right]^{-1}$. The asymptotic expansion for the case $h_1 = h$ reads

$$\sigma^2 = 4\frac{(\boldsymbol{\Omega k})^2}{k^2} \pm 4\frac{\mathcal{N}}{c_{\rm SFL}k}\frac{\sqrt{(k^2 - k_r^2)}}{k^3}(\boldsymbol{\Omega k})\sqrt{\Omega^2k^2 - (\boldsymbol{\Omega k})^2} + O\left(\frac{\mathcal{N}^2}{c_{\rm SFL}^2k^2}\right), \tag{73}$$

where the '+' sign refers to i^s-mode, and the '−' sign refers to the i^0-mode. The frequencies of normal and superfluid i-modes coincide up to the first order in $\mathcal{N}/(c_{\rm SFL}k)$; indeed, one can see in Fig. 1, that the frequencies of $l_0 - m = 3$ and $l_0 - m = 5$ i^s-modes in the case $Y_{\rm np} = 0$ are very close to the corresponding i^0-modes at low temperatures $T \ll T_{\rm cn}$. Fig. 2 also illustrates this point: when protons become non-superfluid (at $T > T_{\rm cp}$), the entrainment effect vanishes and, while temperature is still much less than $T_{\rm cn}$, i^s-modes and i^0-modes with same l_0 are close to each other.

Now let us examine the behaviour of inertial modes in the limit of high temperatures $T \to T_{\rm cn}$. Since the quantity y in this limit tends to infinity, $y \to \infty$, the 'superfluid' speed tends to zero, $c_{\rm SFL} \to 0$. The Brunt-Väisälä frequency, on the other hand, does not depend on temperature. Thus, the ratio $\mathcal{N}/(c_{\rm SFL}k)$ can approach arbitrarily large values, and asymptotic expansions (71)-(73) are invalid. In the limit $c_{\rm SFL}k/\mathcal{N} \ll 1$ asymptotic expansion for the dispersion relation reads

$$\sigma^2 = 4\frac{c_{\rm SFL}^2k^2}{\mathcal{N}^2}\frac{(\boldsymbol{\Omega k})^4}{\Omega^2k^2\,(k^2 - k_r^2)} + O\left(\frac{c_{\rm SFL}^4k^4}{\mathcal{N}^4}\right), \tag{74}$$

$$\sigma^2 = 4\left(\frac{h_1}{h}\right)^2\Omega^2 - 4\frac{c_{\rm SFL}^2k^2}{\mathcal{N}^2}\frac{\left[\Omega^2k^2 - (\boldsymbol{\Omega k})^2\right]\left[(\frac{h_1}{h})^2\Omega^2k^2 - (\boldsymbol{\Omega k})^2\right]}{\Omega^2k^2\,(k^2 - k_r^2)} + O\left(\frac{c_{\rm SFL}^4k^4}{\mathcal{N}^4}\right). \tag{75}$$

Here we see that normal and superfluid modes, described by equations (74) and (75) respectively, exhibit qualitatively different properties at $T \to T_{\rm cn}$: i^0-mode frequencies vanish[6], whereas i^s-mode frequencies have finite values. One can clearly observe such behaviour in Fig. 1 and Fig. 2.

To sum up, in this section we obtained dispersion relations for normal and superfluid inertial modes in superfluid *npe* matter in a short wavelength limit. We analyzed this relations in two opposite limiting cases. The first case, $c_{\rm SFL}k/\mathcal{N} \gg 1$,

[5] We remind the reader that the wavenumber k is assumed to be large; in particular, it is much greater than the inverse stellar radius, $k \gg 1/R = 8.2 \times 10^{-7}$ cm^{-1}.

[6] We remind the reader that we are considering only pure i-modes with $\sigma \propto \Omega$ at low rotation frequencies; in barotropic ($\mathcal{N} = 0$) star normal inertial modes survive at $T > T_{\rm cn}$, since they always have frequency $\sigma^2 = 4(\boldsymbol{\Omega k})^2/k^2$, (see Eqs. 71 and 73 with $\mathcal{N} = 0$). In non-superfluid non-barotropic stars inertial modes (except for the single r-mode) do not exist, since in the limit $\Omega \to 0$ they turn into g-modes (Unno et al. 1989). Therefore it is not surprising that i^0-modes at $T \to T_{\rm cn}$.

That is why $\sigma \to 0$ at $T \to T_{\rm cn}$ in Eq. (74).

describes behaviour of inertial modes at low temperatures $T \ll T_{\rm cn}$. The corresponding relations are presented by Eqs. (71)-(72) (if the entrainment effect is present, $h_1 \neq h$) and Eq. (73) (if $h_1 = h$). These relations explain why the frequencies of superfluid i^s-modes are close to frequencies of the corresponding normal i^0-modes if the entrainment effect is small or absent. The second case, $c_{\rm SFL}k/\mathcal{N} \ll 1$, corresponds to the limit $T \to T_{\rm cn}$, in which i^0-mode frequencies (Eq. 74) tend to zero, while i^s-mode frequencies (Eq. 75) remain finite. These conclusions are consistent with the properties of inertial modes spectrum calculated in Section 4 (see Fig. 1 and Fig. 2).

7 SUMMARY

We calculated the spectrum of $l_0 - |m| = 1$, $l_0 - |m| = 3$, and $l_0 - |m| = 5$ inertial modes for $m = 2$ in slowly rotating superfluid *npe* NSs, working in the leading order in rotation and including for the first time both effects of entrainment and finite temperatures. We present in Section 4 the first results of such calculations. We worked in Newtonian limit (but with relativistic EOS and equilibrium configuration) and assumed that critical temperatures for baryon superfluidity are constant throughout the core.

The main goal of the calculations is to find possible avoided-crossings in the plane 'mode frequency - stellar temperature' between the normal r^0-mode and superfluid inertial modes, i^s-modes. At stellar temperatures corresponding to avoided-crossings, eigenfunctions of r^0-mode and i^s-mode mix with each other. It stabilizes the r^0-mode and provides an explanation of hot and rapidly rotating NSs in LMXBs Gusakov et al. (2014a,b). In our simplified physical model we did not find any avoided-crossing of r^0-mode with superfluid modes in the leading order in rotation frequency. However, we obtained that at temperatures close to the critical temperature of neutrons one should expect stabilizing interaction of r^0-mode with superfluid r^s-mode independently of the details of the physical model employed. Moreover, in our particular model we found that at low temperatures $l_0 - |m| = 3$ i^s-mode has frequency rather close to the r^0-mode frequency and may also stabilize r^0-mode. Further we are going to calculate the spectrum within more accurate models, taking into account muons and realistic critical temperature profiles.

To simplify calculations we have developed an approximate method for calculation of r^s-mode eigenfrequency. In absence of entrainment normal and superfluid r-modes are purely toroidal and have the same frequency in the leading order in Ω (Andersson & Comer 2001; Lee & Yoshida 2003; Andersson et al. 2009; Kantor & Gusakov 2017), but next-order approximation removes this degeneracy, and these modes exhibit avoided crossings at certain resonance temperatures (Kantor & Gusakov 2017). However, the entrainment effect significantly shifts the frequency of supefluid r-mode (see Figs. 1–2), and has to be taken into account. In the present paper we calculated superfluid r-mode analytically in the limit of small entrainment (see Section 5), assuming *npe* core composition and working in the leading order in Ω only. We found a good agreement with the results obtained from the numerical code. This analytical method is similar that of Kantor & Gusakov (2017). In future works we are going to combine both methods, accounting for both first-order entrainment and next-to-leading order in Ω effects. This will allow to calculate avoided crossings between normal and superfluid r-modes (and, thus, r-mode instability windows) under more realistic assumptions.

Also in Section 6 we present and discuss dispersion relations for normal and superfluid inertial modes in superfluid *npe* matter in a short wavelength limit. With a help of these relations we explain some properties of inertial modes in the limits of both low ($T \ll T_{\rm cn}$) and high ($T \to T_{\rm cn}$) temperatures, that can be observed in the numerical results calculated in Section 4.

8 ACKNOWLEDGMENTS

This work is partially supported by the Foundation for the Advancement of Theoretical Physics BASIS [Grant No. 17-12-204-1].

REFERENCES

Akmal A., Pandharipande V. R., Ravenhall D. G., 1998, Phys. Rev. C, 58, 1804
Andersson N., 1998, ApJ, 502, 708
Andersson N., Comer G. L., 2001, MNRAS, 328, 1129
Andersson N., Kokkotas K. D., 2001, International Journal of Modern Physics D, 10, 381
Andersson N., Sidery T., Comer G. L., 2006, MNRAS, 368, 162
Andersson N., Glampedakis K., Haskell B., 2009, Phys. Rev. D, 79, 103009
Friedman J. L., Morsink S. M., 1998, ApJ, 502, 714
Gusakov M. E., 2016, Phys. Rev. D, 93, 064033
Gusakov M. E., Andersson N., 2006, Mon. Not. R. Astron. Soc., 372, 1776
Gusakov M. E., Dommes V. A., 2016, Phys. Rev. D, 94, 083006
Gusakov M. E., Chugunov A. I., Kantor E. M., 2014a, Phys. Rev. D, 90, 063001

Gusakov M. E., Chugunov A. I., Kantor E. M., 2014b, Physical Review Letters, 112, 151101
Gusakov M. E., Haensel P., Kantor E. M., 2014c, MNRAS, 439, 318
Haskell B., Degenaar N., Ho W. C. G., 2012, MNRAS, 424, 93
Heiselberg H., Hjorth-Jensen M., 1999, ApJ, 525, L45
Ho W. C. G., Andersson N., Haskell B., 2011, Physical Review Letters, 107, 101101
Kantor E. M., Gusakov M. E., 2011, Phys. Rev. D, 83, 103008
Kantor E. M., Gusakov M. E., 2017, MNRAS, 469, 3928
Landau L. D., Lifshitz E., 1987, Fluid mechanics. Course of theoretical physics. Pergamon Press, Oxford
Lee U., Yoshida S., 2003, ApJ, 586, 403
Lindblom L., Ipser J. R., 1999, Phys. Rev. D, 59, 044009
Lindblom L., Mendell G., 2000, Phys. Rev. D, 61, 104003
Lockitch K. H., Friedman J. L., 1999, ApJ, 521, 764
Mahmoodifar S., Strohmayer T., 2013, preprint, (arXiv:1302.1204)
Mendell G., 1991, ApJ, 380, 515
Potekhin A. Y., Fantina A. F., Chamel N., Pearson J. M., Goriely S., 2013, A&A, 560, A48
Prix R., Comer G. L., Andersson N., 2002, A&A, 381, 178
Reisenegger A., Goldreich P., 1992, ApJ, 395, 240
Saio H., 1982, ApJ, 256, 717
Unno W., Osaki Y., Ando H., Saio H., Shibahashi H., 1989, Nonradial oscillations of stars
Yoshida S., Lee U., 2000, ApJS, 129, 353